Available online at www.sciencedirect.com
SCIENCE DIRECT®
International Journal of Solids and Structures 43 (2006) 1357–1371
INTERNATIONAL JOURNAL OF SOLIDS and STRUCTURES
www.elsevier.com/locate/ijsolstr

Free vibration analysis of stiffened laminated plates

Guanghui Qing [a,*], Jiajun Qiu [b], Yanhong Liu [a]

[a] Aeronautical Mechanics and Avionics Engineering College, Civil Aviation University of China, Tianjin 300300, People's Republic of China
[b] Department of Mechanics and Engineering Measurement, School of Mechanical Engineering, Tianjin University, 92, Weijin Road, Tianjin 300072, People's Republic of China

Received 23 January 2004; accepted 4 March 2005
Available online 12 April 2005

Abstract

Based on the semi-analytical solution of the state-vector equation theory, a novel mathematical model for free vibration analysis of stiffened laminated plates is developed by separate consideration of plate and stiffeners. The method accounts for the compatibility of displacements and stresses on the interface between the plate and stiffeners, the transverse shear deformation, and naturally the rotary inertia of the plate and stiffeners. Meanwhile, there is no restriction on the thickness of plate and the height of stiffeners. To demonstrate the excellent predictive capability of the model, several examples are analyzed numerically. The model presented in this paper can also be easily modified to solve the problems of stiffened piezolaminated plates and shells, or plates and shells with piezoelectric material patches.

Keywords: Free vibration; Laminated plates; Variational principle; State-vector equation; Semi-analytical solution

1. Introduction

Conventional metal material stiffened plates are structural components consisting of plates reinforced by a system of ribs or beams to enhance their load-carrying capacity. There are many practical applications of such structures. Many stiffened plates are designed to resist vibration due to dynamical loads; the effect of the stiffeners on the vibration behaviors of plates is known to be significant. Thus it is not surprising that a number of papers have been devoted to the study of this problem. Mukherjee and Mukhopadhyay (1986), Mukhopadhyay and Mukherjee (1989) have surveyed different approaches for vibration analysis of

* Corresponding author. Tel.: +86 2224093144; fax: +86 2287401979.
E-mail address: Qingluke@126.com (G. Qing).

0020-7683/$ - see front matter
doi:10.1016/j.ijsolstr.2005.03.012

conventional stiffened plate problems. Many of these approaches can be employed together with the finite element method (FEM). Five main types of finite element models can be identified (Mukherjee and Mukhopadhyay, 1986; Mukhopadhyay and Mukherjee, 1989; Holopainen, 1995). The most common method used in early literature did not account for the effect of transverse shear deformation and the rotary inertia in both the plate and stiffeners (Liew et al., 1995).

Because the laminated plates or shells with stiffeners or stringers become more and more important in the aerospace industry and other modern engineering fields, wide attention has been paid on the experimental, theoretical and numerical analysis for the static and dynamic problems of such structures in recent years. Turkmen and Mecitoglu (1999) presented a numerical analysis and experimental study of stiffened laminated plates exposed to blast shock waves. Zhao et al. (2002), using an energy approach, investigated the free vibration of the stiffened simply supported rotating cross-ply laminated cylindrical shells. Sadek and Tawfik (2000) presented a higher-order finite element model and studied the behavior of concentrically and eccentrically stiffened laminated plates. Kumar and Mukhopadhyay (2000), mixing plane stress triangular element and discrete Kirchhoff–Mindlin plate bending element, investigated the stiffened laminated composite plates. Gong and Lam (1998), using layered shell elements for both plate and stiffener in MSC/Patran and LS-DYNA3D, carried out the transient response analysis of a stiffened composite submersible hull. Rikards et al. (2001) developed triangular finite element and studied the free vibrations of stiffened laminated composite shells. Guo et al. (2002) developed a layerwise finite element formulation and made a buckling analysis of stiffened laminated plates.

In recent years, many investigators have used the state-vector equation to analyze elasticity problem, and particularly, to treat the problems in anisotropic materials and multi-layered structures. Generally speaking, the state-vector equation for elastic bodies can be derived from the field equation or the various variational principles (Steele and Kim, 1992; Chandrashekara and Santhosh, 1990; Fan and Ye, 1990a,b,c; Ding and Tang, 1997, 1999; Zou, 1994; Zou and Tang, 1995a,b; Sheng and Ye, 2002a,b, 2003). The state-vector equation for elastic bodies, derived from the modified mixed Hellinger–Reissner (H–R) variational principle, has been found being in the form of the canonical equations of Hamilton (Steele and Kim, 1992). Hence, some investigators call the state-vector equation as Hamilton canonical equation (Zou, 1994; Zou and Tang, 1995a,b). The state-vector equation can then be solved either analytically or numerically, namely the exact solutions (Steele and Kim, 1992; Chandrashekara and Santhosh, 1990; Fan and Ye, 1990a,b,c; Ding and Tang, 1997) and the semi-analytical finite element solution (Zou, 1994; Zou and Tang, 1995a,b; Sheng and Ye, 2002a,b, 2003). One of the features of the modified mixed H–R variational principle or the corresponding state-vector equation is that the stresses and displacements, which are of immediate interest, are treated simultaneously as the components of the six-dimensional state vector (Steele and Kim, 1992). The prominent advantages using the state-vector equation to handle composite laminates are the varying material and geometric properties along the independent spatial variable are allowed, and anisotropic layered materials can be handled (Steele and Kim, 1992). Another outstanding advantage is to treat the thick plate or multi-layered plate problems. Because of the transfer matrix method being employed, the number of variables in the equation has no relationship with the thickness and/or the number of layers of structures, and the solution also provides a continuous transverse stress field across the thickness of a multi-layered structure (Zou and Tang, 1995a; Sheng and Ye, 2002a,b).

In this paper, a novel mathematical model for the free vibration analysis of stiffened laminated plates is presented. On the basis of the state-vector equation theory, the algebraic equation of plate and stiffeners are established separately. Both the plate and stiffeners are considered as two three-dimensional elastic bodies. Uniting the equations of plate and stiffeners ensures the compatibility of displacements and stresses on the interface between plate and stiffeners. The transverse shear deformation and the rotary inertia are also considered in the model, and the thickness of plate and the height of stiffeners are not restricted. In section three, several numerical examples are analyzed, and the convergence of all examples is tested.

2. The formulation of stiffened laminated plate

A concentrically stiffened laminated plate is shown in Fig. 1.

Assuming the orthotropic symmetry with respect to the coordinate planes (Fig. 1b shows the coordinate system), the stress–displacement relationships of the material of stiffened laminated plate can be stated as

$$\begin{Bmatrix} \sigma_x \\ \sigma_y \\ \sigma_z \\ \tau_{yz} \\ \tau_{xz} \\ \tau_{xy} \end{Bmatrix} = \begin{bmatrix} C_{11} & C_{12} & C_{13} & 0 & 0 & 0 \\ & C_{22} & C_{23} & 0 & 0 & 0 \\ & & C_{33} & 0 & 0 & 0 \\ & & & C_{44} & 0 & 0 \\ & \text{(SYM.)} & & & C_{55} & 0 \\ & & & & & C_{66} \end{bmatrix} \begin{Bmatrix} \alpha u \\ \beta v \\ \gamma w \\ \gamma v + \beta w \\ \alpha w + \gamma u \\ \beta u + \alpha v \end{Bmatrix} \tag{1}$$

where the symbols σ_x, σ_y, σ_z, τ_{yz}, τ_{xz}, and τ_{xy} are the stress components, respectively. $C_{ij}(i,j = 1,2,\ldots,6)$ denotes the elasticity coefficient of material and $\alpha = \partial/\partial x$, $\beta = \partial/\partial y$, $\gamma = \partial/\partial z$. u, v, and w are the displacements in x, y and z directions, respectively.

The modified mixed H–R variational principle (Zou and Tang, 1995a,b) can be shown in the form

$$\delta \prod = \delta\left(\int\int\int_V (\mathbf{p}^{\mathrm{T}} \cdot \dot{\mathbf{q}} - H)\,\mathrm{d}x\,\mathrm{d}y\,\mathrm{d}z - \int\int_{S_\sigma} \mathbf{q}^{\mathrm{T}} \cdot (\mathbf{T} - \overline{\mathbf{T}})\,\mathrm{d}s_\sigma - \int\int_{S_u} \mathbf{T}^{\mathrm{T}} \cdot (\mathbf{q} - \bar{\mathbf{q}})\,\mathrm{d}s_u \right) \tag{2}$$

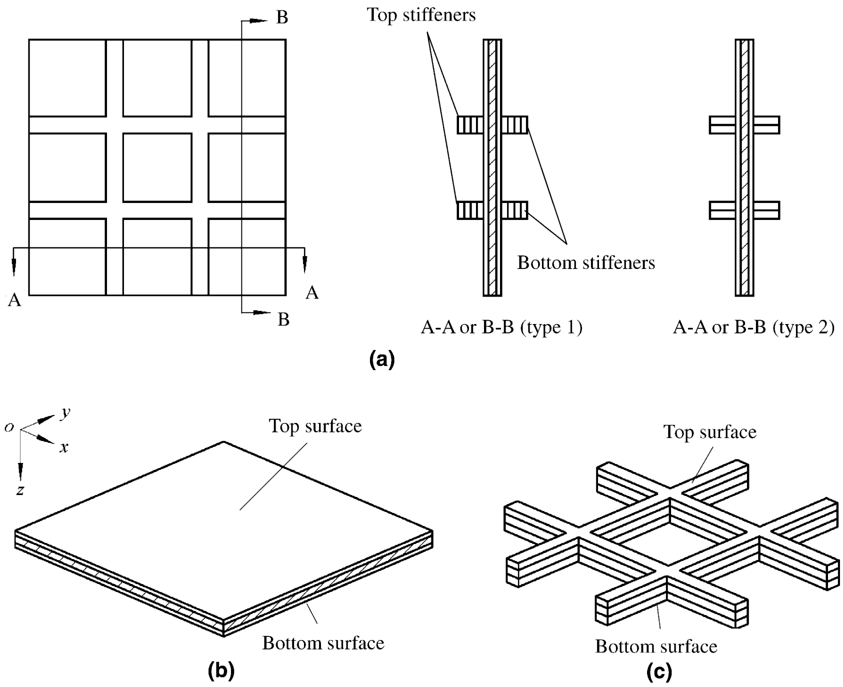

Fig. 1. A concentrically stiffened laminated plate with four stiffeners (a) A concentrically stiffened laminated plate with four stiffeners, (b) laminated plate and (c) top stiffeners or bottom stiffeners.

where

$$\mathbf{q} = [u \quad v \quad w]^{\mathrm{T}}, \quad \mathbf{p} = [\tau_{xz} \quad \tau_{yz} \quad \sigma_z]^{\mathrm{T}}, \quad \dot{\mathbf{q}} = \partial\mathbf{q}/\partial z, \quad \mathbf{T} = [T_x \quad T_y \quad T_z]^{\mathrm{T}}$$

$\overline{\mathbf{T}} = [\overline{T}_x \quad \overline{T}_y \quad \overline{T}_z]^{\mathrm{T}}$ represents the described stresses acting on the stress boundaries S_σ;

$\bar{\mathbf{q}} = [\bar{u} \quad \bar{v} \quad \bar{w}]^{\mathrm{T}}$ represents the described displacements acting on the displacement boundaries S_u;

The expression of the Hamiltonian function H herein can be written as (Body force is neglected)

$$\begin{aligned} H = & -\frac{1}{2}C_2(\alpha u)^2 - C_3\beta v\alpha u + C_1\sigma_z\alpha u - \frac{1}{2}C_4(\beta v)^2 - \frac{1}{2}C_6(\beta u)^2 - \frac{1}{2}C_6(\beta v)^2 + C_6\beta u\alpha v + \frac{1}{2}C_8\tau_{xz}^2 \\ & + \frac{1}{2}C_9\tau_{yz}^2 + C_5\sigma_z\beta v + \frac{1}{2}C_7\sigma_z^2 - \tau_{xz}\beta w - \tau_{yz}\beta w + \frac{1}{2}\rho\omega^2u^2 + \frac{1}{2}\rho\omega^2v^2 + \frac{1}{2}\rho\omega^2w^2 \end{aligned} \tag{3}$$

where ρ is the mass density and ω is the natural frequency.

$$\begin{aligned} & C_1 = -C_{13}/C_{33}, \quad C_2 = C_{11} - C_{13}^2/C_{33}, \quad C_3 = C_{12} - C_{13}C_{23}/C_{33}, \quad C_4 = C_{22} - C_{23}^2/C_{33}, \\ & C_5 = -C_{23}/C_{33}, \quad C_6 = C_{66}, \quad C_7 = 1/C_{33}, \quad C_8 = 1/C_{55}, \quad C_9 = 1/C_{44} \end{aligned}$$

The laminated plate (as shown in Fig. 1b) is considered as an n-layered plate. Using the quadrilateral element (Fig. 2 shows the local coordinate system of the quadrilateral element), the field functions and the shape functions are assumed as follows:

$$\begin{aligned} & u = [\mathbf{N}(x,y)]\{\mathbf{u}^e(z)\}, \quad v = [\mathbf{N}(x,y)]\{\mathbf{v}^e(z)\}, \quad w = [\mathbf{N}(x,y)]\{\mathbf{w}^e(z)\} \\ & \tau_{xz} = [\mathbf{N}(x,y)]\{\boldsymbol{\tau}_{xz}(z)\}, \quad \tau_{yz} = [\mathbf{N}(x,y)]\{\boldsymbol{\tau}_{yz}^e(z)\}, \quad \sigma_z = [\mathbf{N}(x,y)]\{\boldsymbol{\sigma}_z^e(z)\} \end{aligned} \tag{4}$$

$$\mathbf{N}_i(\xi,\eta) = \frac{1}{4}(1+\xi_i\xi)(1+\eta_i\eta) \quad (i = 1,2,\ldots,4) \tag{5}$$

The discretization is employed in the x–y plane of a layer (as shown in Fig. 3a, and the shaded part is the interface of plate and stiffeners).

Assuming the stress boundaries are satisfied ($\mathbf{T} = \overline{\mathbf{T}}$), and the displacement boundaries are satisfied ($\mathbf{q} = \bar{\mathbf{q}}$). Substituting Eqs. (4) and (5) into Eq. (2), with using $\delta\prod = 0$ yields element state-vector equation

$$\mathbf{C}^e\frac{\partial\mathbf{H}^e(z)}{\partial z} = \mathbf{K}^e\mathbf{H}^e(z) \tag{6}$$

The detailed forms of $\mathbf{C}^e$, $\mathbf{K}^e$, $\mathbf{H}^e(z)$ in Eq. (6) can be found in Appendix A.

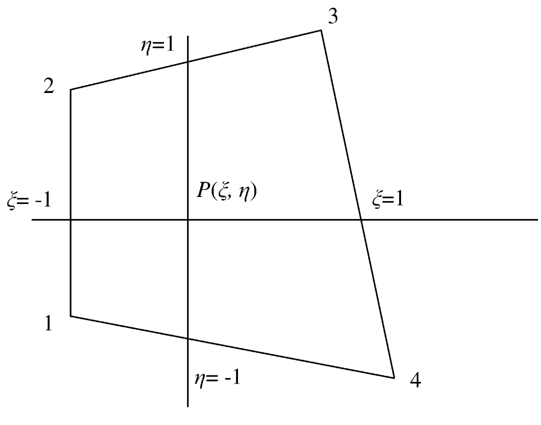

Fig. 2. The local coordinate system of quadrilateral element.

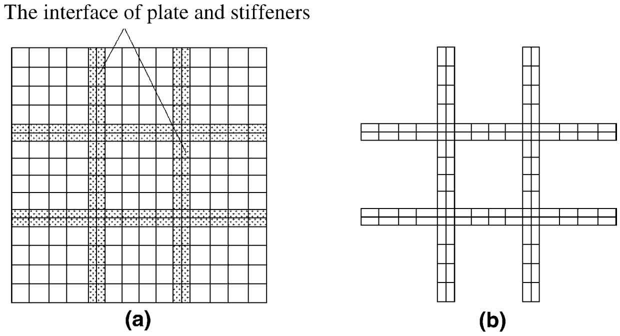

Fig. 3. Element mesh of plate and stiffeners where the shaded part is the interface of plate and stiffeners. (a) The element meshes of plate and (b) the element meshes of stiffeners.

The standard finite element assemblage process is employed. Hence the global state-vector equation for mth layer can be obtained

$$\mathbf{C}_m \frac{\partial \mathbf{H}_m(z)}{\partial z} = \mathbf{K}_m \mathbf{H}_m(z) \tag{7}$$

The exact solution of Eq. (7) is

$$\mathbf{H}_m(z) = \mathbf{T}_m(z)\mathbf{H}_m(0) \tag{8}$$

Note that, $\mathbf{T}_m(z)$ in Eq. (8) usually equals to $\mathrm{e}^{\mathbf{C}_m\mathbf{K}_m\cdot z}$, and the exponential of a matrix could be computed in many ways such as approximation theory, differential equations, the matrix eigenvalues, and the matrix characteristics polynomial and so on. In practice, the consideration of computational stability, efficiency and accuracy indicates that some of the methods are preferable to others, but none is completely satisfactory (Moler and Van, 1978). Hence, the precise integration method (Zhong and Zhu, 1996; Zhong, 2001) for Eq. (7) is employed in this paper.

In fact, Eq. (8) is available to every layer of a laminated plate, the continuity conditions between jth layer and $(j+1)$th layer can be met by imposing following relations at each interface:

$$\mathbf{H}_j(z_j) = \mathbf{H}_{j+1}(z_j) \quad (j = 1, 2, \ldots, n-1) \tag{9}$$

Therefore, the following recursive formation for an n-layered plate can be obtained:

$$\mathbf{H}_n(z_n) = \left(\prod_{j=1}^{n} T_j\right)\mathbf{H}_1(0) \tag{10}$$

Eq. (10) is the relationship of the physics quantities of top and bottom surface of an n-layered plate. As matter of fact, it is a set of linear algebraic equations in terms of the node displacements and stresses. The matrix form of Eq. (10) can be written as

$$\begin{Bmatrix} \mathbf{q}_n(z_n^p) \\ \mathbf{p}_n(z_n^p) \end{Bmatrix} = \begin{bmatrix} \mathbf{T}_{11}^p & \mathbf{T}_{12}^p \\ \mathbf{T}_{21}^p & \mathbf{T}_{22}^p \end{bmatrix} \begin{Bmatrix} \mathbf{q}_1(0^p) \\ \mathbf{p}_1(0^p) \end{Bmatrix} \tag{11a}$$

where superscript p denotes the laminated plate.

The laminated stiffeners (as shown in Fig. 1c) are also considered as an l-layered plate, and assuming the element mesh in every layer is the same as the shaded part of Fig. 3a. The same procedure above for the top stiffeners and bottom stiffeners is performed, and yields following equations:

$$\begin{Bmatrix} \mathbf{q}_l(z_l^{ts}) \\ \mathbf{p}_l(z_l^{ts}) \end{Bmatrix} = \begin{bmatrix} \mathbf{T}_{11}^{ts} & T_{12}^{ts} \\ \mathbf{T}_{21}^{ts} & \mathbf{T}_{22}^{ts} \end{bmatrix} \begin{Bmatrix} \mathbf{q}_1(0^{ts}) \\ \mathbf{p}_1(0^{ts}) \end{Bmatrix} \tag{11b}$$

$$\begin{Bmatrix} \mathbf{q}_l(z_l^{bs}) \\ \mathbf{p}_l(z_l^{bs}) \end{Bmatrix} = \begin{bmatrix} \mathbf{T}_{11}^{bs} & \mathbf{T}_{12}^{bs} \\ \mathbf{T}_{21}^{bs} & \mathbf{T}_{22}^{bs} \end{bmatrix} \begin{Bmatrix} \mathbf{q}_1(0^{bs}) \\ \mathbf{p}_1(0^{bs}) \end{Bmatrix} \tag{11c}$$

where superscript ts and bs denote the top stiffeners and the bottom stiffeners, respectively.

It should be noted that the dimensionality of Eqs. (11b) or (11c) is not equal to that of Eq. (11a).

The displacements and stresses on the interface between plate and stiffeners must be continuous. Uniting Eqs. (11a)–(11c) yields

$$\begin{Bmatrix} \mathbf{q}(z) \\ \mathbf{p}(z) \end{Bmatrix} = \begin{bmatrix} \mathbf{T}_{11} & \mathbf{T}_{12} \\ \mathbf{T}_{21} & \mathbf{T}_{22} \end{bmatrix} \begin{Bmatrix} \mathbf{q}(0) \\ \mathbf{p}(0) \end{Bmatrix} \tag{12}$$

Because natural frequencies are studied here, the top surface and bottom surface are stress free (the stress column vector $\mathbf{p}(z) = \mathbf{p}(0) = 0$), the following equation can be deduced from Eq. (12):

$$\mathbf{T}_{21}\mathbf{q}(0) = 0 \tag{13}$$

To obtain the nontrivial solutions of Eq. (13), the determinant of the characteristic matrix in Eq. (13) must be zero, namely

$$|\mathbf{T}_{21}| = 0 \tag{14}$$

The natural frequencies ω can be obtained from characteristic polynomial of Eq. (14) through the use of the bisection method (Johnston, 1982). For the purpose of simplifying the analysis and the accuracy of results, the dimensionless quantities of u, v, w, τ_{xz}, τ_{yz}, and σ_z need to be introduced in computer program.

3. Numerical examples and discussions

To illustrate the versatility of the current method, numerical computations have been performed by using Maple® and Matlab®.

3.1. Verification of the proposed method

An aluminum alloy eccentrically stiffened plate with double stiffeners (Fig. 4), which is a previously reported experimental and theoretical example (Olson and Hazell, 1977; Zeng and Bert, 2001), is selected as the first example to validate present method.

Because the compatible finite elements in the x–y plane are used, the natural frequencies should converge on the values of the mathematical model monotonically, as the number of elements in the discretization is increased. The results, as listed in Table 1, show that reasonable convergence has been achieved with relatively small decrements in the first four frequencies, never as much as 1%, between corresponding value for mesh $42 \times 42,1$ and mesh $51 \times 51,1$.

It is obvious (see Table 2) that the first three modes are in good agreement with other authors' results, but for the fourth mode the natural frequency is under-predicted in comparison to the experimental result. The same situation was mentioned in reference (Olson and Hazell, 1977). The reasons need to be further investigated, but it is clear that the fourth mode is in an agreement with the corresponding result of FEM (Olson and Hazell, 1977) and DQ (Zeng and Bert, 2001). It can be also noticed that the natural frequencies obtained using present method are lower than those of FEM (Olson and Hazell, 1977). In the FEM (Olson and Hazell, 1977), the plate portion of the stiffened panels was modeled with triangular ele-

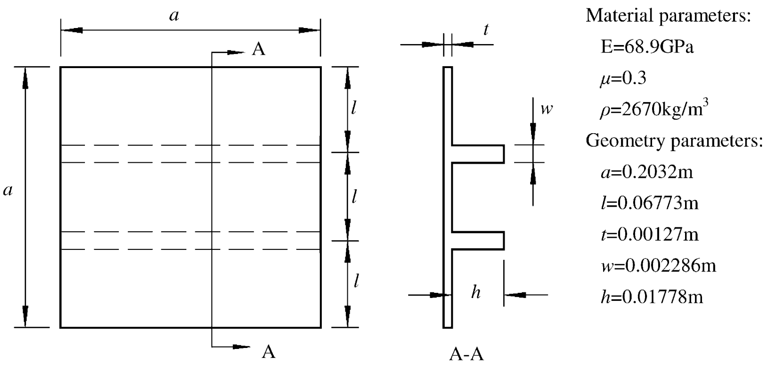

Fig. 4. An eccentrically stiffened plate with double stiffeners.

Table 1
Convergence of natural frequencies (Hz) for eccentrically stiffened plate with double stiffeners and clamped at edges

Mesh ($k \times m$), layer (n)		Mode number			
Plate	Stiffeners	1	2	3	4
11×11, 1	1×11, 8	1020.4	1360.2	1482.8	1679.9
22×22, 1	2×22, 8	941.5	1234.3	1359.2	1430.1
33×33, 1	2×33, 8	932.7	1223.1	1334.7	1422.8
42×42, 1	2×42, 8	931.6	1221.4	1332.6	1410.1
51×51, 1	2×51, 8	931.5	1220.9	1331.8	1403.3

Table 2
Comparison of natural frequencies (Hz) for eccentrically stiffened plate with double stiffeners and clamped at edges

Methods	Mode number (error % = 100 × (Present-Ref.)/Ref.)			
	1	2	3	4
Experimental, Olson and Hazell (1977)	909 (2.475)	1204 (1.404)	1319 (0.970)	1506 (−6.819)
FEM, Olson and Hazell (1977)	965.3 (−3.501)	1272.3 (−4.040)	1364.3 (−2.382)	1418.1 (−1.044)
DQ[a], Zeng and Bert (2001)	915.9 (1.703)	1242.2 (−1.715)	1344.4 (0.937)	1414.1 (−0.764)
Present	931.5	1220.9	1331.8	1403.3

[a] Differential quadrature method.

ments and the stiffeners were modeled by refined beam bending and torsion elements. Both in-plane and bending motions in the plate were considered, but in-plane inertias were neglected. However, without any assumption for plate and stiffeners, the transverse shear deformation, the rotary inertia of plate and stiffeners are considered in the present method. It is obvious that the current model is more advanced.

In the following subsections, several new numerical examples have been analyzed.

3.2. The natural frequencies of stiffened laminated plates

As shown in Fig. 5, the plate has two identical face layers and a core layer. All three layers have the material properties corresponding to Aragonite crystals (Srinivas and Rao, 1970; Fan and Ye, 1990c) that have the following stiffness ratios.

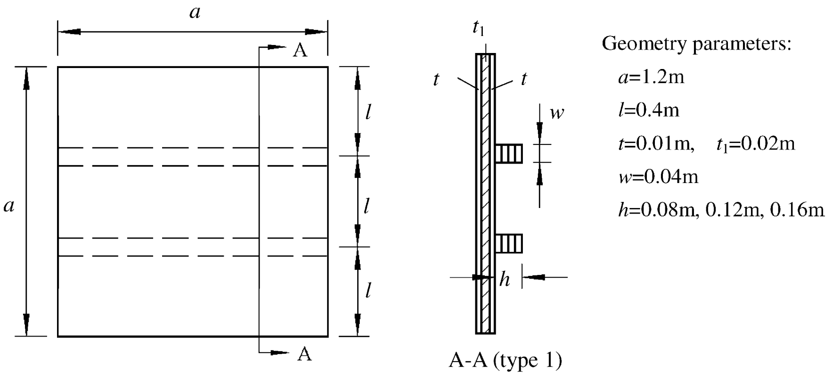

Fig. 5. An eccentrically stiffened laminated plate with double stiffeners $C_{22}/C_{11} = 0.543103$, $C_{12}/C_{11} = 0.23319$, $C_{23}/C_{11} = 0.098276$, $C_{13}/C_{11} = 0.010776$, $C_{33}/C_{11} = 0.530172$, $C_{44}/C_{11} = 0.26681$, $C_{55}/C_{11} = 0.159914$, $C_{66}/C_{11} = 0.262931$.

Table 3
The natural frequencies (Hz) for eccentrically stiffened laminated plate with double stiffeners and clamped at edges

h (m)	Mesh ($k \times m$), layer (n)		Mode number			
	Plate	Stiffeners	1	2	3	4
0.08	33 × 33, 4	3 × 33, 8	554.6	897.2	1184.5	1490.8
	42 × 42, 4	3 × 42, 8	554.4	895.7	1181.8	1487.1
	51 × 51, 4	3 × 51, 8	554.3	895.4	1179.7	1485.9
	60 × 60, 4	3 × 60, 8	554.2	895.2	1178.4	1484.8
0.12	33 × 33, 4	3 × 33, 12	660.4	943.2	1389.2	1393.1
	42 × 42, 4	3 × 42, 12	659.9	941.8	1385.3	1389.9
	51 × 51, 4	3 × 51, 12	659.6	941.5	1382.8	1387.9
	60 × 60, 4	3 × 60, 12	659.4	941.1	1382.1	1386.5
0.16	33 × 33, 4	3 × 33, 16	748.2	992.6	1165.4	1386.8
	42 × 42, 4	3 × 42, 16	747.9	991.7	1163.5	1384.3
	51 × 51, 4	3 × 51, 16	747.4	991.0	1160.1	1380.1
	60 × 60, 4	3 × 60, 16	747.3	990.9	1159.7	1379.4

Assuming $C^1_{11} = 150$ GPa and $\rho^1 = 1600$ kg/m^3 for the two face layers C^2_{11} and ρ^2 for the core layer of the laminated plate, $C^1_{11}/C^2_{11} = 2$, $\rho^1/\rho^2 = 2$ and the material properties of stiffeners are the same as those of the face layers. The numerical results are listed in Table 3.

The first four mode shapes (h at 0.08 m, 0.12 m, and 0.16 m) are depicted in Fig. 6.

The numerical results in Table 3 show that the natural frequencies of the first two modes increase with the increase of height of stiffeners. However, it is not true for the third mode and the fourth mode. For the third mode, the natural frequency increases at first, and then decreases. For the fourth mode, the natural frequency decreases with the increase of height of stiffeners. It is reasonable because the effect of the inertia terms becomes more prominent for the higher modes with the increase of stiffener height. This situation can also be explained by the mode shapes. The fourth mode shapes are shown by Fig. 6d, h and l when h at 0.08 m, 0.12 m, and 0.16 m, respectively. Actually, the fourth mode shape changes at different stiffener height because of the strong effect of the inertia.

In the third example, as shown in Fig. 7, the material and the geometry parameters of every layer and stiffeners are the same as those in example two, except the height of top and bottom stiffeners is a half of that of example two ($h_1 = h/2$). The numerical results are listed in Table 4.

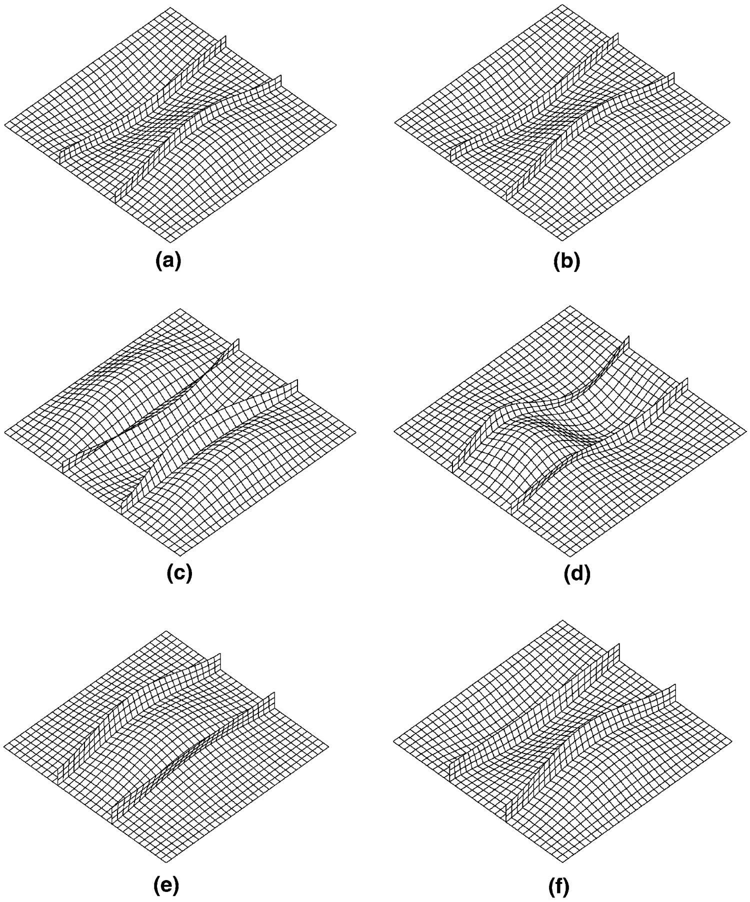

Fig. 6. Mode shapes of an eccentrically stiffened laminated plate with double stiffeners. (a) Mode shape 1 ($h = 0.08$ m, 554.2 Hz), (b) Mode shape 2 ($h = 0.08$ m, 895.2 Hz), (c) Mode shape 3 ($h = 0.08$ m, 1178.4 Hz), (d) Mode shape 4 ($h = 0.08$ m, 1484.8 Hz), (e) Mode shape 1 ($h = 0.12$ m, 659.4 Hz), (f) Mode shape 2 ($h = 0.12$ m, 941.1 Hz), (g) Mode shape 3 ($h = 0.12$ m, 1382.1 Hz), (h) Mode shape 4 ($h = 0.12$ m, 1386.5 Hz), (i) Mode shape 1 ($h = 0.16$ m, 747.3 Hz), (j) Mode shape 2 ($h = 0.16$ m, 990.9 Hz), (k) Mode shape 3 ($h = 0.16$ m, 1159.7 Hz) and (l) Mode shape 4 ($h = 0.16$ m, 1379.4 Hz).

The numerical results in Table 4 show that the natural frequencies of the first three modes increase with the increase of stiffener height. For the fourth mode, the natural frequency increases at first, and then decreases. This situation is the same as example two. The same case can be found in the following example four (see Table 5).

Based on the treatment of the eccentricity of the stiffeners, the previous works on free vibration of conventional eccentrically stiffened plates can be divided into two groups (Harik and Guo, 1993). In the first group, the eccentricity of the stiffeners is neglected. In the second group, the in-plate displacements are introduced as independent degrees of freedom to treat the actual plate-eccentric stiffeners system. Consequently, the location of the neutral surfaces is not required to determine the membrane force in the plate element and the axial force in the stiffener. The present method falls into the second group.

If the eccentricity of stiffened laminated plate is neglected and the neutral surface (see Fig. 8) is assumed to coincide with the middle surface of the plate and the centroidal axis of the stiffeners, example two can be modeled by example three. The natural frequencies of modes 1 and 2 of example three are lower than those of example two.

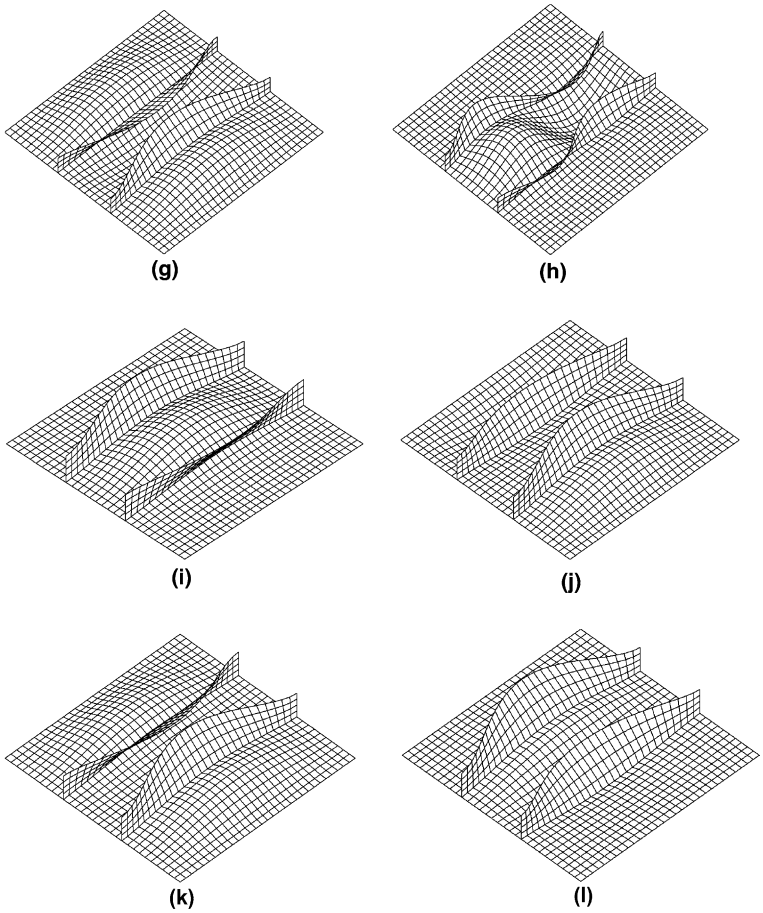

Fig. 6 (*continued*)

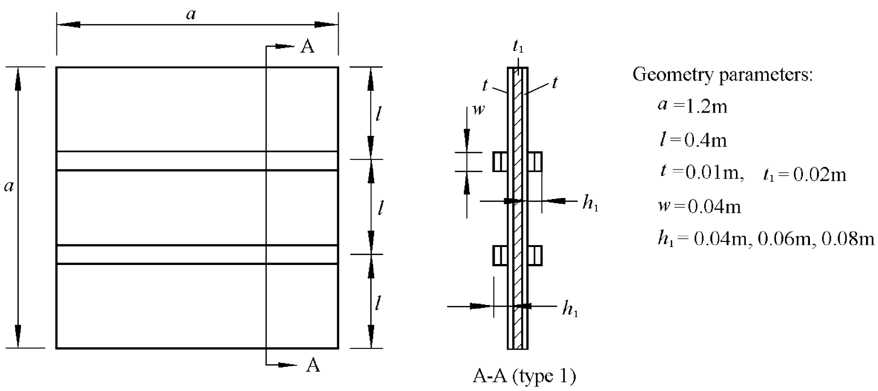

Fig. 7. A concentrically stiffened laminated plate with double stiffeners.

The fourth example is relatively complicated (see Fig. 9), the eccentrically stiffened laminated plate with four T type stiffeners. The plate has two identical face layers and a core layer. The material properties of

Table 4
The natural frequencies (Hz) for concentrically stiffened laminated plate with double stiffeners and clamped at edges

h_1 (m)	Mesh ($k \times m$), layer (n)		Mode number			
	Plate	Stiffeners	1	2	3	4
0.04	33×33, 4	3×33, 4	502.2	867.1	1083.3	1395.5
	42×42, 4	3×42, 4	501.8	865.5	1080.4	1391.8
	51×51, 4	3×51, 4	501.3	865.2	1078.9	1390.7
	60×60, 4	3×60, 4	501.1	865.0	1078.1	1389.6
0.06	33×33, 4	3×33, 6	583.1	884.2	1290.6	1558.7
	42×42, 4	3×42, 6	582.5	882.7	1286.9	1554.3
	51×51, 4	3×51, 6	582.4	882.4	1284.8	1552.8
	60×60, 4	3×60, 6	583.4	881.8	1284.1	1552.2
0.08	33×33, 4	3×33, 8	670.9	922.7	1465.4	1504.3
	42×42, 4	3×42, 8	669.8	922.6	1460.5	1498.1
	51×51, 4	3×51, 8	669.1	921.2	1456.6	1495.4
	60×60, 4	3×60, 8	669.1	921.1	1456.5	1495.2

Table 5
The natural frequencies (Hz) for eccentrically stiffened laminated plate with four T type stiffeners and clamped at edges

h (m)	Mesh ($k \times m$), layer (n)			Mode number			
	Plate	Webs	Flange	1	2	3	4
0.08	32×32, 3	2×32, 8	4×32, 2	810.7	1319.3	1490.2	1998.4
	44×44, 3	2×44, 8	4×44, 2	809.6	1314.6	1484.4	1988.1
	53×53, 3	2×53, 8	4×53, 2	809.4	1313.9	1481.9	1986.6
	62×62, 3	2×62, 8	4×62, 2	809.3	1313.6	1481.7	1986.2
0.12	32×32, 3	2×32, 12	4×32, 2	956.1	1501.1	1674.5	2207.1
	44×44, 3	2×44, 12	4×44, 2	955.4	1496.6	1669.0	2196.8
	53×53, 3	2×53, 12	4×53, 2	955.6	1495.8	1666.8	2195.9
	62×62, 3	2×62, 12	4×62, 2	955.5	1495.4	1666.3	2195.2
0.16	32×32, 3	2×32, 16	4×32, 2	1073.7	1637.5	1813.3	2141.7
	44×44, 3	2×44, 16	4×44, 2	1072.2	1634.3	1810.4	2135.7
	53×53, 3	2×53, 16	4×53, 2	1072.1	1634.0	1808.2	2131.5
	62×62, 3	2×62, 16	4×62, 2	1072.0	1633.9	1807.9	2131.3

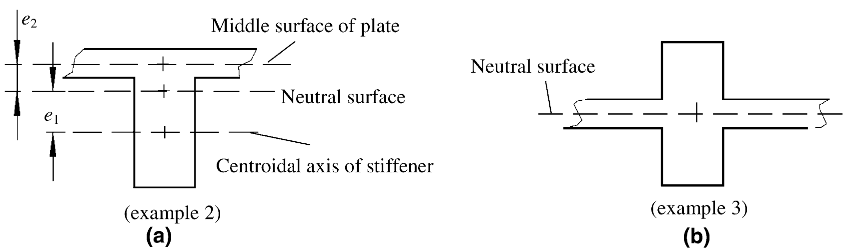

Fig. 8. (a) Plate and eccentric stiffener and (b) eccentricity of stiffener is neglected.

every layer and stiffeners are the same as those in example two. The convergence patterns with different meshes are tabulated in Table 5. The natural frequencies, as expected, converge from above and reach an acceptable bound result.

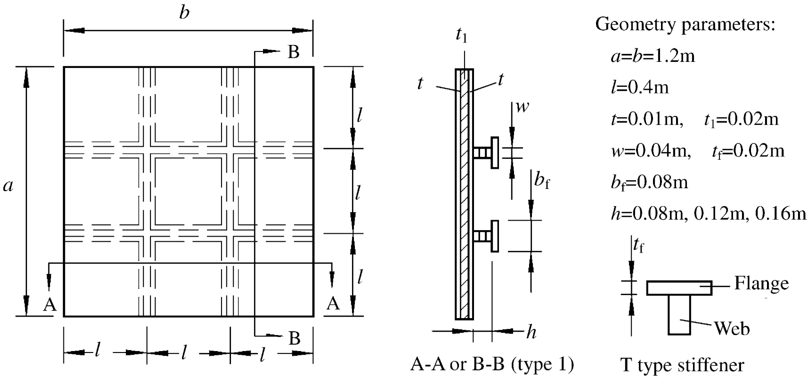

Fig. 9. An eccentrically stiffened laminated plate with four T type stiffeners.

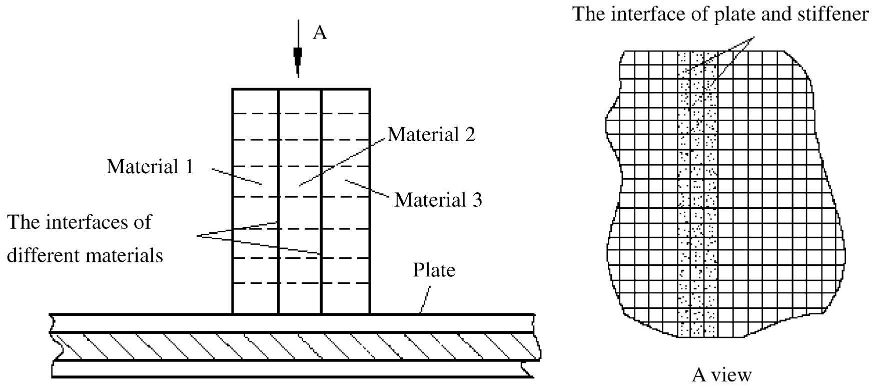

Fig. 10. The stiffener type 2.

It should be mentioned that, if the cross-section of the stiffener is rectangular, the node number of a layer of laminated plate determines the number of variables in Eq. (12), that is, the number of variables included in Eq. (12) has no relationship with the thickness or the number of stiffeners of structures (examples 1–3). But if the cross-section of stiffener is T type or Γ type, lateral parts of web should add the number of variables in the model analyzed (example 4).

On the other hand, in all numerical examples, the stiffener type is 1 and the material is the same over the cross-section. If there are two or more materials in the cross-section of the stiffener, the present method is also suitable for this situation without additional equations. This is because Eq. (11a) can be used to handle the laminated plates that the material of every layer can be different.

If the stiffener type 2 (Figs. 1a and 10) is concerned, the laminated stiffener (as shown in Fig. 10) is considered as an n-layered plate and there are two or more materials in a layer. This situation is also similar to the stiffener type 1. The major difference is that we should notice the interfaces of different materials when we discretize arbitrary layer of the stiffener. One element cannot include two or more materials.

4. Conclusions

In this study, a novel mathematical model for the free vibration analysis of stiffened laminated plates has been developed. The algebraic equations of the plate and the stiffeners have been established separately.

The major advantages of the developed model include: (1) the compatibility of displacements and stresses on the interface between the plate and the stiffeners are ensured through uniting the algebraic equation of the plate and the stiffeners, (2) the transverse shear deformation and the rotary inertia are considered naturally in the model, (3) the thickness of plates and the height of stiffeners are not limited.

The model can also be easily modified to solve the static or dynamic problems of plates with discontinuity in thickness. If the similar modified H–R mixed variational principle for piezoelectric materials and corresponding discrete state-vector equation are established, the dynamic behaviors of piezoelectric plate with piezoelectric patches and cylindrical shells with piezoelectric rings (Lee and Saravanos, 1997; Lin et al., 1996; Wang et al., 1997) can be analyzed directly by using the present approach.

Acknowledgments

This work was supported by the National Natural Science Foundation of China (Grant No. 10072038). The authors would like to express their thanks to both reviewers for their valuable comments.

Appendix A

The expressions of $\mathbf{C}^e$, $\mathbf{K}^e$, $\mathbf{H}^e$ in Eq. (6):

$$\mathbf{C}^e = \mathrm{diag}\left(\int\int_{\Omega e} \mathbf{N}_i\mathbf{N}_j|\mathbf{J}|\,\mathrm{d}\xi\,\mathrm{d}\eta\right)$$

$$\mathbf{H}^e(z) = \begin{bmatrix} \mathbf{u}^e(z) & \mathbf{v}^e(z) & \mathbf{w}^e(z) & \boldsymbol{\tau}^e_{xz}(z) & \boldsymbol{\tau}^e_{yz}(z) & \boldsymbol{\sigma}^e_z(z) \end{bmatrix}^{\mathrm{T}}$$

$$= \begin{bmatrix} u_1^e\cdots u_4^e & v_1^e\cdots v_4^e & w_1^e\cdots w_4^e & \tau^e_{xz1}\cdots\tau^e_{xz4} & \tau^e_{yz1}\cdots\tau^e_{yz4} & \sigma^e_{z1}\cdots\sigma^e_{z4} \end{bmatrix}^{\mathrm{T}}$$

$$\mathbf{K}^e = \begin{bmatrix} \mathbf{0} & \mathbf{0} & [\mathbf{K}]^e_{13} & [K]^e_{14} & \mathbf{0} & \mathbf{0} \\ \mathbf{0} & \mathbf{0} & [\mathbf{K}]^e_{23} & \mathbf{0} & [\mathbf{K}]^e_{25} & \mathbf{0} \\ [\mathbf{K}]^e_{31} & [\mathbf{K}]^e_{32} & \mathbf{0} & \mathbf{0} & \mathbf{0} & [\mathbf{K}]^e_{36} \\ [\mathbf{K}]^e_{41} & [\mathbf{K}]^e_{42} & \mathbf{0} & \mathbf{0} & \mathbf{0} & [\mathbf{K}]^e_{46} \\ [\mathbf{K}]^e_{51} & [\mathbf{K}]^e_{52} & \mathbf{0} & \mathbf{0} & \mathbf{0} & [\mathbf{K}]^e_{56} \\ \mathbf{0} & \mathbf{0} & [\mathbf{K}]^e_{63} & [\mathbf{K}]^e_{64} & [\mathbf{K}]^e_{65} & \mathbf{0} \end{bmatrix}$$

$$[\mathbf{K}_{ij}]^e_{13} = -\int\int_{\Omega_e} \mathbf{N}_i\frac{\partial\mathbf{N}_j}{\partial x}|\mathbf{J}|\,\mathrm{d}\xi\,\mathrm{d}\eta, \quad [\mathbf{K}_{ij}]^e_{14} = \int\int_{\Omega_e} C_8\mathbf{N}_i\mathbf{N}_j|\mathbf{J}|\,\mathrm{d}\xi\,\mathrm{d}\eta$$

$$[\mathbf{K}_{ij}]^e_{23} = -\int\int_{\Omega_e} \mathbf{N}_i\frac{\partial\mathbf{N}_j}{\partial y}|\mathbf{J}|\,\mathrm{d}\xi\,\mathrm{d}\eta, \quad [\mathbf{K}_{ij}]^e_{25} = \int\int_{\Omega_e} C_9\mathbf{N}_i\mathbf{N}_j|\mathbf{J}|\,\mathrm{d}\xi\,\mathrm{d}\eta$$

$$[\mathbf{K}_{ij}]^e_{31} = -\int\int_{\Omega_e} \mathbf{N}_i\frac{\partial\mathbf{N}_i}{\partial x}\mathbf{N}_j|\mathbf{J}|\,\mathrm{d}\xi\,\mathrm{d}\eta, \quad [\mathbf{K}_{ij}]^e_{32} = \int\int_{\Omega_e} C_5\frac{\partial\mathbf{N}_i}{\partial y}\mathbf{N}_jd|\mathbf{J}|\,\mathrm{d}\xi\,\mathrm{d}\eta$$

$$[\mathbf{K}_{ij}]^e_{36} = \int\int_{\Omega_e} C_7\mathbf{N}_i\mathbf{N}_j|\mathbf{J}|\,\mathrm{d}\xi\,\mathrm{d}\eta$$

$$[\mathbf{K}_{ij}]^e_{41} = \int\int_{\Omega_e}\left(-\rho\omega^2\mathbf{N}_i\mathbf{N}_j + C_2\frac{\partial\mathbf{N}_i}{\partial x}\frac{\partial\mathbf{N}_j}{\partial x} + C_6\frac{\partial\mathbf{N}_i}{\partial y}\frac{\partial\mathbf{N}_j}{\partial y}\right)|\mathbf{J}|\,\mathrm{d}\xi\,\mathrm{d}\eta$$

$$[\mathbf{K}_{ij}]^e_{42} = \int\int_{\Omega_e}\left(C_3\frac{\partial\mathbf{N}_i}{\partial x}\frac{\partial\mathbf{N}_j}{\partial y} + C_6\frac{\partial\mathbf{N}_i}{\partial y}\frac{\partial\mathbf{N}_j}{\partial x}\right)|\mathbf{J}|\,\mathrm{d}\xi\,\mathrm{d}\eta$$

$$[\mathbf{K}_{ij}]^e_{46} = -\int\int_{\Omega_e} C_1 \frac{\partial \mathbf{N}_i}{\partial x}\mathbf{N}_j|\mathbf{J}|\,\mathrm{d}\xi\,\mathrm{d}\eta, \quad [\mathbf{K}_{ij}]^e_{51} = \int\int_{\Omega_e}\left(C_6 \frac{\partial \mathbf{N}_i}{\partial x}\frac{\partial \mathbf{N}_j}{\partial y} + C_3 \frac{\partial \mathbf{N}_i}{\partial y}\frac{\partial \mathbf{N}_j}{\partial x}\right)|\mathbf{J}|\,\mathrm{d}\xi\,\mathrm{d}\eta$$

$$[\mathbf{K}_{ij}]^e_{52} = \int\int_{\Omega_e}\left(-\rho\omega^2\mathbf{N}_i\mathbf{N}_j + C_6 \frac{\partial \mathbf{N}_i}{\partial x}\frac{\partial \mathbf{N}_j}{\partial x} + C_4 \frac{\partial \mathbf{N}_i}{\partial y}\frac{\partial \mathbf{N}_j}{\partial y}\right)|\mathbf{J}|\,\mathrm{d}\xi\,\mathrm{d}\eta$$

$$[\mathbf{K}_{ij}]^e_{56} = -\int\int_{\Omega_e} C_5 \frac{\partial \mathbf{N}_i}{\partial y}\mathbf{N}_j|\mathbf{J}|\,\mathrm{d}\xi\,\mathrm{d}\eta, \quad [\mathbf{K}_{ij}]^e_{63} = \int\int_{\Omega_e} -\rho\omega^2\mathbf{N}_i\mathbf{N}_j|\mathbf{J}|\,\mathrm{d}\xi\,\mathrm{d}\eta$$

$$[\mathbf{K}_{ij}]^e_{64} = \int\int_{\Omega_e} \frac{\partial \mathbf{N}_i}{\partial x}\mathbf{N}_j|\mathbf{J}|\,\mathrm{d}\xi\,\mathrm{d}\eta \quad [\mathbf{K}_{ij}]^e_{65} = \int\int_{\Omega_e} \frac{\partial \mathbf{N}_i}{\partial y}\mathbf{N}_j|\mathbf{J}|\,\mathrm{d}\xi\,\mathrm{d}\eta$$

in which

$$\mathbf{J} = \begin{bmatrix} \sum_{i=1}^4 \frac{\partial \mathbf{N}_i}{\partial \xi} x_i & \sum_{i=1}^4 \frac{\partial \mathbf{N}_i}{\partial \xi} y_i \\ \sum_{i=1}^4 \frac{\partial \mathbf{N}_i}{\partial \eta} x_i & \sum_{i=1}^4 \frac{\partial \mathbf{N}_i}{\partial \eta} y_i \end{bmatrix}, \quad \begin{Bmatrix} \partial/\partial x \\ \partial/\partial y \end{Bmatrix} = \mathbf{J}^{-1}\begin{Bmatrix} \partial/\partial \xi \\ \partial/\partial \eta \end{Bmatrix}$$

References

Chandrashekara, S., Santhosh, U., 1990. The natural frequencies of cross-ply laminates by state space approach. Journal of Sound and Vibration 136, 413–424.

Ding, K.W., Tang, L.M., 1997. Exact analysis for axisymmetric vibration and buckling of the thick laminated closed cylindrical shells in a Hamilton system. Journal of Sound and Vibration 206, 435–441.

Ding, K.W., Tang, L.M., 1999. Three-dimensional free vibration of thick laminated cylindrical shells with clamped edges. Journal of Sound and Vibration 220, 171–177.

Fan, J.R., Ye, J.Q., 1990a. Exact solutions for axisymmetric vibration of laminated circular plate. Journal of Engineering Mechanics ASCE 116, 920–927.

Fan, J.R., Ye, J.Q., 1990b. A series solution of the exact equation for thick orthotropic plates. International Journal of Solids and Structures 26, 773–778.

Fan, J.R., Ye, J.Q., 1990c. An exact solution for the statics and dynamics of laminated thick plates with orthotropic layers. International Journal of Solids and Structures 26, 655–662.

Gong, S.W., Lam, K.Y., 1998. Transient response of stiffened composite sub-mersible hull subjected to underwater explosive shock. Composite Structures 41, 27–37.

Guo, M.W., Harik, I.E., Ren, W.X., 2002. Buckling behavior of stiffened laminated plates. International Journal of Solids and Structures 39, 3039–3055.

Harik, I.E., Guo, M.W., 1993. Finite element analysis of eccentrically stiffened plates in free vibration. Computers and Structures 49, 1007–1015.

Holopainen, T.P., 1995. Finite element free vibration analysis of eccentrically stiffened plates. Computers and Structures 56, 993–1007.

Johnston, R.L., 1982. Numerical Methods. John Wiley, New York.

Kumar, S.Y.V., Mukhopadhyay, M., 2000. A new triangular stiffened plate element for laminate analysis. Composites Science and Technology 60, 935–943.

Lee, H.J., Saravanos, D.A., 1997. Generalized finite element formulation for smart multilayered thermal piezoelectric composite plates. International Journal Solids and Structures 34, 3355–3371.

Liew, K.M., Xiang, Y., Kitipornchai, S., Meek, J.L., 1995. Formulation of Mindlin–Engesser model for stiffened plate vibration. Computer Methods in Applied Mechanics and Engineering 120, 339–353.

Lin, C.C., Hsu, C.Y., Huang, H.N., 1996. Finite element analysis on deflection control of plates with piezoelectric actuators. Composite Structures 35, 423–433.

Moler, C., Van, L.C., 1978. Nineteen dubious ways to compute the exponential of a matrix. SIAM Review (Society for Industrial and Applied Mathematics) 20, 801–836.

Mukherjee, A., Mukhopadhyay, M., 1986. A review of dynamic behavior of stiffened plates. The Shock and Vibration Digest 18, 3–8.

Mukhopadhyay, M., Mukherjee, A., 1989. Recent advances on the dynamic behavior of stiffened plates. The Shock and Vibration Digest 21, 6–9.

Olson, M.D., Hazell, C.R., 1977. Vibration studies on some integral rib-stiffened plates. Journal of Sound and Vibration 50, 43–61.

Rikards, R., Chate, A., Ozolinsh, O., 2001. Analysis for buckling and vibrations of composite stiffened shells and plates. Composite Structures 51, 361–370.
Sadek, E.A., Tawfik, S.A., 2000. A finite element model for the analysis of stiffened laminated plates. Computers and Structures 75, 369–383.
Sheng, H.Y., Ye, J.Q., 2002a. A state space finite element for laminated composite plates. Computer Methods in Applied Mechanics and Engineering 191, 4259–4276.
Sheng, H.Y., Ye, J.Q., 2002b. A semi-analytical finite element for laminated composite plates. Computers and Structures 57, 117–123.
Sheng, H.Y., Ye, J.Q., 2003. A three-dimensional state space finite element solution for laminated composite cylindrical shells. Computer Methods in Applied Mechanics and Engineering 192, 2441–2459.
Srinivas, S., Rao, A.K., 1970. Bending vibration and buckling of simply supported thick orthotropic rectangular plate and laminates. International Journal of Solids and Structures 6, 1463–1481.
Steele, C.R., Kim, Y.Y., 1992. Modified mixed variational principle and the state-vector equation for elastic bodies and shells of revolution. Journal of Applied Mechanics 59, 587–595.
Turkmen, H.S., Mecitoglu, Z., 1999. Dynamic response of a stiffened laminated composite plates subjected to blast load. Journal of Sound and Vibration 221, 371–389.
Wang, X.M., Ehlers, C., Neitzel, M., 1997. An analytical investigation of static model of piezoelectric patches attached to beams and plates. Smart Material Structures 6, 204–213.
Zeng, H., Bert, C.W., 2001. A differential quadrature analysis of vibration for rectangular stiffened plates. Journal of Sound and Vibration 241, 247–252.
Zhao, X., Liew, K.M., Ng, T.Y., 2002. Vibrations of rotating cross-ply laminated circular cylindrical shells with stringer and rings stiffeners. Journal of Solids and Structures 39, 529–545.
Zhong, W.X., Zhu, J.P., 1996. Precise time integration for the matrix Riccati differential equation. Journal on Numerical Methods in Computer Applications 17, 26–35.
Zhong, W.X., 2001. Combined method for the solution of asymmetric Riccati differential equation. Computer Methods in Applied Mechanics and Engineering 191, 93–102.
Zou, G.P., 1994. The mixed state equation, Hamilton canonical equation and a semi-analytical solution for the analysis of laminated composite plates and shells (in Chinese). Ph.D. Thesis. Dalian University of Technology.
Zou, G.P., Tang, L.M., 1995a. A semi-analytical solution for thermal stress analysis of laminated composite plates in the Hamiltonian system. Computers and Structures 55, 113–118.
Zou, G.P., Tang, L.M., 1995b. A semi-analytical solution for laminated composite plates in Hamilton system. Computer Methods in Applied Mechanics and Engineering 128, 395–404.